JOURNAL OF Materials CHEMISTRY

Transport properties and thermoelectric performance of $(Zn_{1-y}Mg_y)_{1-x}Al_xO$

Toshiki Tsubota, Michitaka Ohtaki, Koichi Eguchi* and Hiromichi Arai

Department of Materials Science and Technology, Graduate School of Engineering Science, Kyushu University, 6–1 Kasugakoen, Kasuga, Fukuoka 816 Japan

Addition of MgO to Al-doped ZnO was successful in reduction of the phonon thermal conductivity, κ_{ph}, in order to suppress the unfavorably high thermal conductivity, κ, of the material in terms of applications to thermoelectric conversion. The electrical conductivity, σ, of $Zn_{0.98}Al_{0.02}O$ decreased with increasing amount of the added MgO, whereas the Seebeck coefficient was virtually unchanged up to $(Zn_{0.9}Mg_{0.1})_{0.98}Al_{0.02}O$. Further Al_2O_3 doping was ineffective in improving σ. The carrier mobility decreased with increasing amount of the added MgO but was independent of the extent of the Al doping. In spite of the significant suppression of κ, the figure of merit was smaller for the MgO-added samples because of the marked decrease of σ.

Thermoelectric power generation converts thermal energy directly to electrical energy *via* the Seebeck effect in solid materials. This technique has been considered to be very promising for improvement in energy conversion efficiency, because it should be effective in utilizing waste heat as a power source. In the last three decades, Si–Ge alloys,[1] several metal chalcogenides,[2,3] transition-metal disilicides,[4–6] some boron compounds,[7,8] and skutterudites and filled skutterudites[9–11] have been developed as materials for high-temperature thermoelectric power generation. However, the materials so far developed have still some problems in practical use; many are highly expensive and even require costly surface protection to prevent oxidation or vaporization; some others have inherent temperature limits owing to phase transitions at high temperatures.

The thermoelectric figure of merit, Z, which evaluates thermoelectric performance of materials, is defined as

$$Z = S^2\sigma/\kappa$$

where σ is the electrical conductivity, S is the Seebeck coefficient and κ is the thermal conductivity. Whereas practical applications generally require $Z \geqslant 1 \times 10^{-3}$ K^{-1}, larger temperature difference across the thermoelectric devices also improves the conversion efficiency. The dimensionless figure of merit, ZT (T is average operation temperature), is hence regarded as the most comprehensive criterion.

With respect to high-temperature operation in air, metal oxides in their common oxidation states should apparently be advantageous owing to their excellent stability to heat. Moreover, rather many oxide materials are reported to have high electrical conductivities. Refractory metal oxide semiconductors would therefore be worth investigating in their applicability to high temperature thermoelectric energy conversion because of their high thermal stability and corrosion resistance.

We have already reported the thermoelectric properties of several promising oxides, such as In_2O_3–SnO_2,[12] $CaMnO_3$,[13,14] $(Zn_{1-x}Al_x)O$[15–17] and $(Zn_{1-x}M_x)O$ (M = Ga, In).[18] Very recently, some other oxide materials such as $(ZnO)_mIn_2O_3$,[19,20] $CdIn_2O_4$[21] and $Nd_{2-x}Ce_xCuO_4$[22] appeared in the literature in terms of thermoelectric conversion. However, most of these materials suffer from poorer electrical properties compared to conventional thermoelectric materials, and this might be difficult to overcome since a drastic (one order or more) reduction of κ is generally unlikely.

In previous papers, we have reported that $(Zn_{1-x}Al_x)O$ exhibits a very large power factor ($S^2\sigma$), which evaluates the electrical component of the thermoelectric performance, and that it also shows unfavorably high κ values in terms of thermoelectric applications.[15–17] In spite of the high κ values, the Z values of $(Zn_{1-x}Al_x)O$ were still promising, benefiting from the large power factors. Reduction of κ without seriously affecting $S^2\sigma$ is therefore required for improvement in Z values of $(Zn_{1-x}Al_x)O$.

We have already revealed that the lattice thermal conductivity, κ_{ph}, dominantly contributes to overall κ of $(Zn_{1-x}Al_x)O$.[15–17] If phonon scattering centers can be effectively introduced without scattering the charge carriers, then Z values of these materials will be greatly improved. Enhancement of the phonon scattering by point defects induced by formation of solid solutions has been known to be efficient to reduce κ_{ph}. Substitution of lattice points by isovalent heteroatoms would be expected to enhance selective phonon scattering.

However, very few elements dissolve in ZnO to a substantial extent. Exceptionally, it is known that the solubility limit of MgO in ZnO is $>10\%$.[23] Moreover, Mg ions are divalent similarly to Zn, implying that the MgO dissolved in ZnO would not affect the carrier concentration in ZnO. Here, we report the thermoelectric and transport properties of $(Zn_{1-x}Al_x)O$ incorporating MgO.

Experimental

Sintered samples of $(Zn_{1-y}Mg_y)_{1-x}Al_xO$ ($x = 0$–0.1, $y = 0$–0.1) were prepared from powders of ZnO, Al_2O_3 and MgO of guaranteed grade. The powders were mixed and pulverized in a nylon-lined ball mill for 24 h. The powder mixture was pressed into a pellet and sintered at 1400 °C for 10 h in air. The heating and cooling rate was 200 °C h^{-1}. The crystal phases in the samples thus obtained were determined from a powder X-ray diffraction (XRD) study using Cu-Kα radiation. Both the electrical conductivity and Seebeck coefficient of each sample were simultaneously measured in air, from room temperature up to 1000 °C. The measurement procedures have been described elsewhere in detail.[12] The thermal conductivity was determined from thermal diffusivity and specific heat capacity measured by the laser flash technique and differential scanning calorimetry (DSC), respectively. The Hall measurements were carried out by the van der Pauw method at room temperature.

Results and Discussion

Transport properties of the $(Zn_{1-y}Mg_y)_{1-x}Al_xO$ system

$(Zn_{1-y}Mg_y)_{0.98}Al_{0.02}O$ system. First, the effect of addition of MgO on the transport properties was investigated for

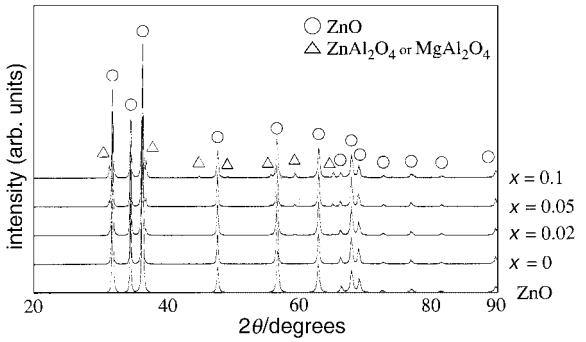

Fig. 1 XRD profiles of $(Zn_{1-y}Mg_y)_{0.98}Al_{0.02}O$ ($y=0$, 0.02, 0.05, 0.1)

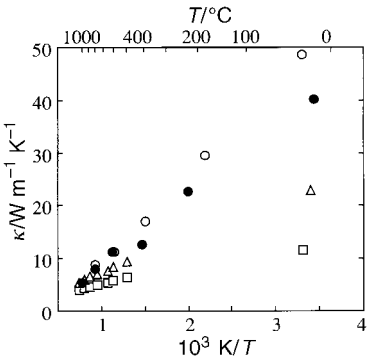

Fig. 2 The thermal conductivities of ZnO (○), $(Zn_{1-y}Mg_y)_{0.98}Al_{0.02}O$ for $y=0$ (●), 0.02 (△), 0.1 (□) as a function of inverse temperature

$Zn_{0.98}Al_{0.02}O$ as a basic composition, since $Zn_{0.98}Al_{0.02}O$ showed the highest Z value in the $Zn_{1-x}Al_xO$ system.[15–17]

It was confirmed by XRD of $(Zn_{1-y}Mg_y)O$ that the solubility limit of MgO in ZnO is >10 mol%. Fig. 1 shows XRD profiles of $(Zn_{1-y}Mg_y)_{0.98}Al_{0.02}O$ ($y=0$, 0.02, 0.05, 0.1). It should be noted that the XRD profiles of these samples were virtually the same, including the sample at $y=0$. The XRD patterns consist of dominant peaks for the ZnO phase accompanied by small peaks for the spinel phase ($ZnAl_2O_4$ or $MgAl_2O_4$), while no MgO phase was detected. The diffraction lines of $MgAl_2O_4$ can hardly be distinguished from those of $ZnAl_2O_4$. However, it is most probable that the peaks due to the spinel phase are attributed to $ZnAl_2O_4$, because these peaks already exist for $Zn_{0.98}Al_{0.02}O$, and their intensity was constant even with the addition of increasing amounts of MgO. We therefore presume that the added MgO completely dissolved in the ZnO lattice.

The inverse temperature dependence of the thermal conductivity for $(Zn_{1-y}Mg_y)_{0.98}Al_{0.02}O$ ($y=0$, 0.02, 0.1) is shown in Fig. 2 in comparison with that for ZnO. Although the κ values of ZnO were almost unchanged by Al-doping of 2 mol%, κ of the sample at $y=0.02$ was considerably lower, and was further decreased with increasing amount of the doped MgO. The difference in κ between the MgO-added samples and $Zn_{0.98}Al_{0.02}O$ is significantly larger at lower temperatures, indicating that the addition of MgO was very effective in reduction of κ at low temperatures.

The thermal conductivity of solid materials consists of the lattice thermal conductivity, κ_{ph}, and the carrier thermal conductivity, κ_{el};

$$\kappa = \kappa_{ph} + \kappa_{el}$$

In order to specify κ_{ph} and κ_{el} in the overall value of κ, κ_{el} was calculated from σ by using the Weidemann–Franz law, $\kappa_{el}=L\sigma T$ (L is the Lorentz number).[24] The lattice thermal conductivity of $(Zn_{1-y}Mg_y)_{0.98}Al_{0.02}O$ ($y=0$, 0.02, 0.1) obtained by subtracting κ_{el} from κ is indicated in Fig. 3 as a function of inverse temperature. It is known that κ_{ph} is proportional to $1/T$ above the Debye temperature (usually

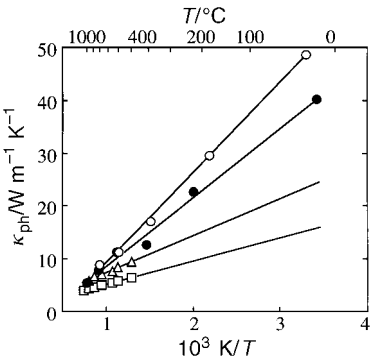

Fig. 3 The phonon thermal conductivities of ZnO (○), $(Zn_{1-y}Mg_y)_{0.98}Al_{0.02}O$ for $y=0$ (●), 0.02 (△), 0.1 (□) as a function of inverse temperature

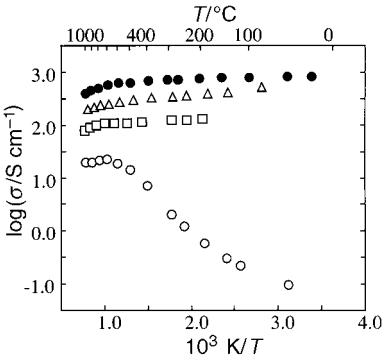

Fig. 4 Arrhenius plots for the electrical conductivities of ZnO (○), $(Zn_{1-y}Mg_y)_{0.98}Al_{0.02}O$ for $y=0$ (●), 0.02 (△), 0.1 (□)

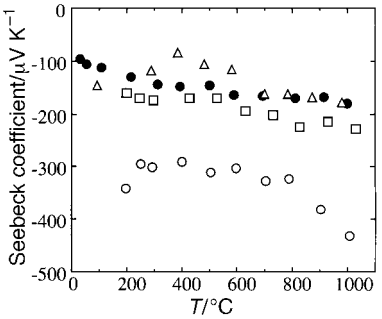

Fig. 5 The Seebeck coefficients of ZnO (○), $(Zn_{1-y}Mg_y)_{0.98}Al_{0.02}O$ for $y=0$ (●), 0.02 (△), 0.1 (□)

below room temperature)[25] and this is clearly confirmed in Fig. 3. It is also obvious that the decrease in κ_{ph} is mainly responsible for the reduction of κ upon addition of MgO. Formation of a solid solution of MgO to ZnO is thereby concluded to be effective in introducing phonon scattering centers in order to reduce κ_{ph}, and thereby the overall value of κ.

The temperature dependences of the electrical conductivity, σ, and the Seebeck coefficient, S, of $(Zn_{1-y}Mg_y)_{0.98}Al_{0.02}O$ ($y=0$, 0.02, 0.1) are shown in Fig. 4 and Fig. 5, respectively. We have already reported that the addition of a small amount of Al_2O_3 in ZnO increased the σ values and changed the σ behavior from semiconducting to metallic.[15–17] The enhancement of σ by Al-doping can be explained by valence control theory. The σ value of $Zn_{0.98}Al_{0.02}O$ decreased with increasing amount of added MgO, but the behavior of σ remained metallic. The S values of all the samples are negative, indicating n-type conduction. The $|S|$ value of ZnO decreased upon Al-doping. However, the addition of MgO to $Zn_{0.98}Al_{0.02}O$ scarcely altered the temperature dependence of the Seebeck coefficient.

Table 1 Transport properties of $(Zn_{1-y}Mg_y)_{1-x}Al_xO$ at room temperature

x	y	$n/10^{25}$ m^{-3}	μ_H/cm^2 V^{-1} s^{-1}	κ/W m^{-1} K^{-1}
0.02	0	7.2	81	43
0.02	0.02	6.4	59	20
0.02	0.5	4.8	50	14
0.02	0.1	6.6	22	8.1
0	0.1	0.17	29	7.2
0.02	0.1	6.6	22	8.1
0.05	0.1	4.3	35	9.3
0.1	0.1	3.3	27	7.2

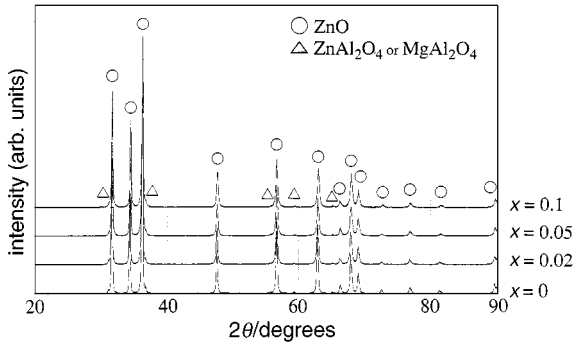

Fig. 6 XRD profiles of $(Zn_{0.9}Mg_{0.1})_{1-x}Al_xO$ ($x=0$, 0.02, 0.05, 0.1)

Although the addition of MgO reduced κ, the σ value was also affected. We have further measured the Hall coefficients to analyze the electrical transport properties. The carrier concentrations, n, the Hall mobilities, μ_H and the thermal conductivities, κ, at room temperature are summarized in Table 1 for $(Zn_{1-y}Mg_y)_{1-x}Al_xO$. The values of both μ_H and κ were inversely correlated with the amount of MgO, while n was independent. The decrease in μ_H should therefore be responsible for the suppression of σ caused by the addition of MgO. The almost unchanged value of n may explain the unchanged S value. These results would lead to a conclusion that the scattering centers introduced by the addition of MgO scattered not only phonons but also carrier electrons to some extent.

$(Zn_{0.9}Mg_{0.1})_{1-x}Al_xO$ system. Although the addition of MgO to ZnO-based oxides was successful in reduction of κ, σ of these materials was also considerably affected. We thus further investigated the optimization of the Al-doping for $(Zn_{0.9}Mg_{0.1})O$ by varying the amount of Al, since at this composition MgO completely dissolves in ZnO, giving the lowest κ in the $(Zn_{1-y}Mg_y)_{0.98}Al_{0.02}O$ system.

The XRD profiles of $(Zn_{0.9}Mg_{0.1})_{1-x}Al_xO$ ($x=0$, 0.02, 0.05, 0.1) are shown in Fig. 6. As seen when varying the Mg content, only two phases were detected in the samples; the ZnO phase and the spinel phase ($ZnAl_2O_4$ or $MgAl_2O_4$). However, in this case, the amount of the spinel phase increased with increasing Al_2O_3 content, strongly suggesting the formation of the $ZnAl_2O_4$ phase. Neither the Al_2O_3 phase nor the MgO phase was detected by XRD.

Arrhenius plots of the electrical conductivity for $(Zn_{0.9}Mg_{0.1})_{1-x}Al_xO$ ($x=0.02$, 0.1), $Zn_{0.98}Al_{0.02}O$, and ZnO are shown in Fig. 7. At $x=0.02$, σ is considerably smaller than for $Zn_{0.98}Al_{0.02}O$. Moreover, σ was slightly suppressed, rather than enhanced, by increasing the amount of the doped Al_2O_3. As shown in Fig. 6, the peaks belonging to the spinel phase increased with increasing the amount of doped Al_2O_3.

Because both $MgAl_2O_4$ and $ZnAl_2O_4$ have high electrical resistivity, the suppression of σ can be attributed to the increase in the amount of the spinel phase. The temperature dependence

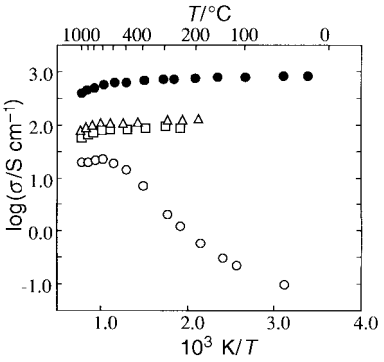

Fig. 7 Arrhenius plots for the electrical conductivities of ZnO (○), $Zn_{0.98}Al_{0.02}O$ (●), $(Zn_{0.9}Mg_{0.1})_{1-x}Al_xO$ for $x=0.02$ (△), 0.1 (□)

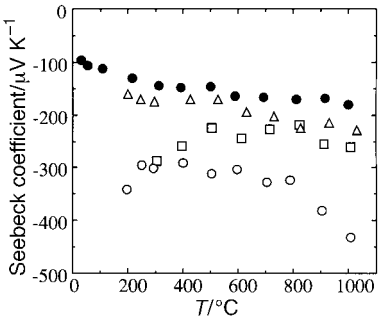

Fig. 8 The Seebeck coefficients of ZnO (○), $Zn_{0.98}Al_{0.02}O$ (●), $(Zn_{0.9}Mg_{0.1})_{1-x}Al_xO$ for $x=0.02$ (△), 0.1 (□)

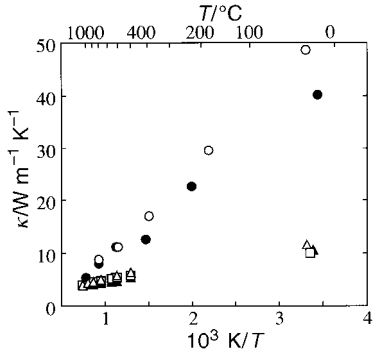

Fig. 9 The thermal conductivities of ZnO (○), $Zn_{0.98}Al_{0.02}O$ (●), $(Zn_{0.9}Mg_{0.1})_{1-x}Al_xO$ for $x=0$ (▲), 0.02 (△), 0.1 (□) as a function of inverse temperature

of the Seebeck coefficients of $(Zn_{0.9}Mg_{0.1})_{1-x}Al_xO$ ($x=0.02$, 0.1), $Zn_{0.98}Al_{0.02}O$ and ZnO is shown in Fig. 8. The $|S|$ value slightly increased with increasing amount of the doped Al_2O_3.

The temperature dependence of the thermal conductivity is shown in Fig. 9 for $(Zn_{0.9}Mg_{0.1})_{1-x}Al_xO$ ($x=0$, 0.02, 0.1), $Zn_{0.98}Al_{0.02}O$ and ZnO. The reduction of κ from ZnO to $Zn_{0.98}Al_{0.02}O$ was almost negligible. The doping of Al_2O_3 is therefore considered to be ineffective in suppressing κ of ZnO based materials.

Values of n and μ_H for ZnO at room temperature were 0.052×10^{25} m^{-3} and 67 cm^2 V^{-1} s^{-1}, respectively. On the other hand, those for $(Zn_{0.9}Mg_{0.1})O$ at room temperature were 0.17×10^{25} m^{-3} and 29 cm^2 V^{-1} s^{-1}, respectively. It should be noted that n increased but μ_H decreased upon addition of MgO. Further Al-doping of $(Zn_{0.9}Mg_{0.1})O$ provided carrier electrons, but left μ_H unchanged. However, the n values slightly decreased, rather than increased, with increasing amount of doped Al_2O_3. The excess Al atoms ($x>0.02$) therefore did not

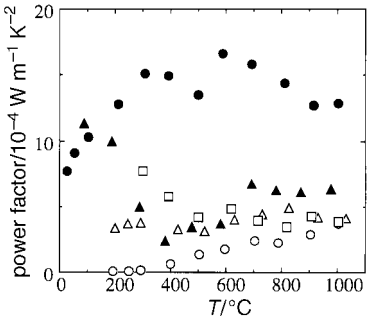

Fig. 10 The power factors of ZnO (○), $(Zn_{0.9}Mn_{0.1})_{0.9}Al_{0.1}O$ (▲), $(Zn_{1-y}Mg_y)_{0.98}Al_{0.02}O$ for $y=0$ (●), 0.02 (△), 0.1 (□)

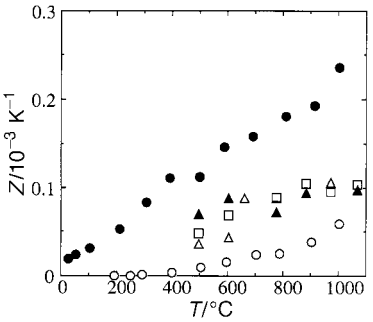

Fig. 11 The figures of merit of ZnO (○), $(Zn_{0.9}Mn_{0.1})_{0.9}Al_{0.1}O$ (▲), $(Zn_{1-y}Mg_y)_{0.98}Al_{0.02}O$ for $y=0$ (●), 0.02 (△), 0.1 (□)

provide electrons. As one can see, not only μ_H but also κ are almost independent of x. These data indicate that Al is ineffective as scattering center for either phonons or carrier electrons. A reciprocal relation between the decrease in σ and the increase in S by excess Al_2O_3 doping may be explained by the decrease in n.

Thermoelectric performance of the $(Zn_{1-y}Mg_y)_{1-x}Al_xO$ system

In order to evaluate the thermoelectric performance of $(Zn_{1-y}Mg_y)_{1-x}Al_xO$, the power factor and the figure of merit were calculated from σ, S and κ obtained above.

The temperature dependence of the power factors of ZnO, $(Zn_{0.9}Mg_{0.1})_{0.9}Al_{0.1}O$ and $(Zn_{1-y}Mg_y)_{0.98}Al_{0.02}O$ ($y=0$, 0.02, 0.1) is shown in Fig. 10. The power factors of all the MgO-added samples are much smaller than that of $Zn_{0.98}Al_{0.02}O$. The suppression of σ is obviously responsible for the decrease in $S^2\sigma$, and is essentially ascribed to the smaller μ_H values of the MgO-added samples compared to ZnO and $Zn_{0.98}Al_{0.02}O$.

Fig. 11 depicts the temperature dependence of the figure of merit for ZnO, $(Zn_{0.9}Mg_{0.1})_{0.9}Al_{0.1}O$ and $(Zn_{1-y}Mg_y)_{0.98}Al_{0.02}O$ ($y=0$, 0.02, 0.1). The Z values of all the MgO-added samples were about one third of that of $Zn_{0.98}Al_{0.02}O$, giving maximum values of *ca.* 0.1×10^{-3} K^{-1} at 1000 °C. The considerable decrease in σ upon addition of MgO to $Zn_{1-x}Al_xO$ prevented an improvement in their thermoelectric performance. The low μ_H values of the MgO-added samples would be responsible for the low Z values. However, the marked suppression of κ was achieved particularly at low temperatures. It is well known that Mg is considerably more electropositive compared to Zn. A large difference in the electronegativity between point defects and the host lattice would also enhance scattering of the carrier electrons and may cause a significant reduction of μ_H. If phonon scattering centers can sufficiently be introduced by dissolving elements more electronegative than Mg, further improvement in Z by selective phonon scattering would be expected.

Conclusions

Transport properties and thermoelectric performance of $(Zn_{1-y}Mg_y)_{1-x}Al_xO$ investigated in the present study revealed that the addition of MgO to ZnO is effective in reducing κ *via* suppression of κ_{ph}. The σ values of $Zn_{0.98}Al_{0.02}O$, however, also decreased with increasing addition of MgO, whereas the S values were almost unchanged. The results of the Hall measurement indicated that the decrease in σ is ascribed to lower carrier mobilities. The excess doping of Al_2O_3 into $(Zn_{0.9}Mg_{0.1})O$ was unsuccessful in recovering the lowered σ, and consequently, $S^2\sigma$ remained smaller than that of $Zn_{0.98}Al_{0.02}O$. Although the figure of merit stayed lower than that of the Al-doped ZnO, the significant reduction of κ was realized by introducing the point defects into the ZnO lattice.

The authors thank Mr.Yasuhiro Yamada of the Government Industrial Research Institute, Kyushu, for his kind cooperation on the laser flash measurement of κ. The DSC measurement of the specific heat capacity was under cooperation of Japan Ultrahigh-Temperature Materials Research Center. This work was financially supported in part by Research Fellowships of the Japan Society for the Promotion of Science for Young Scientists.

References

1 C. M. Bhandari and D. M. Rowe, *Contemp. Phys.*, 1980, **21**, 219.
2 J. C. Bass and N. B. Elsner, in *Proc. 3rd Int. Conf. Therm. Energ. Conv.*, University of Texas, Arlington, 1980, p. 8.
3 J. F. Nakahara, T. Takeshita, M. J. Tschetter, B. J. Beaudry and K. A. Gschneidner Jr., *J.Appl. Phys.*, 1988, **63**, 2331.
4 I. Nishida, *Phys. Rev. B*, 1973, **7**, 2710.
5 I. Nishida and T. Sakata, *J. Phys. Chem. Solids*, 1978, **39**, 499.
6 T. Kojima, *Phys. Status Solidi A*, 1989, **111**, 233.
7 C. Wood and D. Emin, *Phys. Rev. B*, 1984, **29**, 4582.
8 S. Yugo, T. Sato and T. Kimura, *Appl. Phys. Lett.*, 1985, **46**, 842.
9 T. Caillat, A. Borshchevsky and J.-P. Fleurial, in *Proc. 13th Int. Conf. Thermoelectrics*, ed. B. Mathiprakasem, ALP Press, New York, 1994, p. 58.
10 G. S. Nolas, G. A. Slack, D. T. Morelli, T. M. Tritt, A. C. Ehrlich, *J. Appl. Phys.*, 1996, **79**, 4002.
11 A. Borshchevsky, T. Caillat and J.-P. Fleurial, in *Proc. 15th Int. Conf. Thermoelectrics*, 1996, p. 112.
12 M. Ohtaki, D. Ogura, K. Eguchi and H. Arai, *J. Mater. Chem.*, 1994, **4**, 653.
13 M. Ohtaki, H. Koga, T. Tokunaga, K. Eguchi and H. Arai, *J. Solid State Chem.*, 1995, **120**, 105.
14 M. Ohtaki, H. Koga, T. Tokunaga, K. Eguchi and H. Arai, in *Proc. 13th Int. Conf. Thermoelectrics*, ed. B. Mathiprakasem, ALP Press, New York, 1994, p. 115.
15 M. Ohtaki, T. Tsubota, K. Eguchi and H. Arai, *J. Appl. Phys.*, 1996, **79**, 1816.
16 T. Tsubota, M. Ohtaki, K. Eguchi and H. Arai, *J. Mater. Chem.*, 1997, **7**, 85.
17 M. Ohtaki, T. Tsubota, K. Eguchi and H. Arai, in *Proc. 14th Int. Conf. Thermoelectrics*, ed. M. V. Vedernikov, A. F. Ioffe Physical-Technical Institute, St. Petersburg, 1995, p. 245.
18 T. Tsubota, M. Ohtaki, K. Eguchi and H. Arai, in *Proc. 16th Int. Conf. Thermoelectrics*, in press.
19 H. Ohta, W. S. Seo and K. Koumoto, *J. Am. Ceram. Soc.*, 1996, **79**, 2193.
20 H. Hiramatsu, H. Ohta, W. S. Seo and K. Koumoto, *J. Jpn. Soc. Powder Powder Metall.*, 1997, **44**, 44.
21 W. S. Seo, H. Sinmachi and K. Koumoto, *in Proc. of the Annual Meeting of the Ceramic Society of Japan*, Ceramic Society of Japan, Nagoya, 1994, p. 206 (in Japanese).
22 M. Yasukawa, N. Murakami, *J. Jpn. Soc. Powder Powder Metall.*, 1997, **44**, 50.
23 E. R. Segnit and A. E. Holland, *J. Am. Ceram. Soc*, 1965, **48**, 412.
24 M. E. Fine and N. Hsieh, *J. Am. Ceram. Soc.*, 1974, **57**, 502.
25 C. Kittel, in *Introduction to Solid State Physics*, 5th edn., John Wiley & Sons, Inc., New York, 1976.

Paper 7/06213C; *Received* 26*th August*, 1997